# Pyochelin biotransformation shapes bacterial competition

C. Jenul[1], K. Keim[1], J. Jens[2], M. J. Zeiler[3], K. Schilcher[1], M. Schurr[1], C. Melander[3], V.V. Phelan[2] *, A.R. Horswill[1, 4] *

**Affiliations:**

[1] Department of Immunology and Microbiology, School of Medicine, University of Colorado, Anschutz Medical Campus, Aurora, CO, USA

[2] Department of Pharmaceutical Sciences, Skaggs School of Pharmacy and Pharmaceutical Sciences, University of Colorado, Anschutz Medical Campus, Aurora, CO, USA

[3] Department of Chemistry and Biochemistry, University of Notre Dame, Notre Dame, IN, USA

[4] Department of Veterans Affairs, Eastern Colorado Health Care System, Denver, CO, USA

* Corresponding author. Email: alexander.horswill@cuanschutz.edu (ARH)
vanessa.phelan@cuanschutz.edu (VVP)

**Abstract:** It has become evident that numerous infections are polymicrobial and *Pseudomonas aeruginosa* and *Staphylococcus aureus* are among the most frequently isolated co-infecting bacterial species. We applied mass spectrometry guided interaction studies to determine how chemical interaction shapes the fitness and community structure during co-infection of these two pathogens. We demonstrate that *S. aureus* is equipped with an elegant mechanism, inactivation of pyochelin via the yet uncharacterized methyltransferase Spm (staphylococcal pyochelin methyltransferase), to increase its survival during *in vivo* competition with *P. aeruginosa*. Methylation of pyochelin abolishes the siderophore activity of pyochelin and significantly lowers pyochelin-mediated intracellular ROS production in *S. aureus*. In a murine wound co-infection model, a *S. aureus* mutant unable to metyhlate pyochelin shows significant lower fitness compared to its parental strain.

**One-Sentence Summary:** *Staphylococcus aureus* inactivates pyochelin to increase its survival during *in vivo* competition with *Pseudomonas aeruginosa*.

*Staphylococcus aureus* and *Pseudomonas aeruginosa* are frequently co-isolated from lung infections of cystic fibrosis (CF) patients and chronic wound infections (*1-5*) and these co-infections have been associated with worsened patient outcomes (*6, 7*). Despite their frequent co-isolation from infections, co-cultivation under standard laboratory conditions leads to antagonistic interactions between these two microbes with *P. aeruginosa* outcompeting *S. aureus* (*8-12*). *P. aeruginosa* synthesiszes several alkyl-quinolones, of which some regulate the production of anti-staphylococcal factors (*e.g.,* 2-heptyl-4(1H)-quinolone, HHQ; *Pseudomonas* quinolone signal, 2-heptyl-3-hydroxy-4(1H)-quinolone, PQS), like pyocyanin and rhamnolipids, and others directly inhibit *S. aureus* growth (*e.g*., 2-heptyl-4-quinolone-N-oxide, HQNO) (*13-16*). To elucidate the mechanistic underpinning of the interaction between *S. aureus* and *P. aeruginosa in vivo*, most studies have focused on how temporal adaptation to the infection environment mediates their co-existence (*17*). The objective of this study was to identify key metabolic exchange factors in the interaction between non-adapted *P. aeruginosa* and *S. aureus* and uncover the roles for these metabolites in mediating their co-existence *in vivo.*

To determine the metabolite profile of *S. aureus* and *P. aeruginosa* co-cultures, methicillin-resistant *S. aureus* strain (MRSA) LAC USA300 and *P. aeruginosa* strain PAO1 (PAO1) or its alkyl-quinolone deficient derivative PAO1 Δ*pqsA* (**fig. S1**) were grown as an adjacent co-culture on tryptic soy agar (TSA). (**Fig. 1A, fig. S1**) and subjected to matrix-assisted laser desorption ionization mass spectrometry imaging (MALDI-MSI). A mass to charge ratio, *m/z* 339, was exclusively detected in the co-cultures, localized to the MRSA colony, when competing with PAO1 (**Fig. 1A**). Classical molecular networking analysis was applied to untargeted liquid chromatrography tandem mass spectrometry (LC-MS/MS) metabolomics data generated from chemical extracts of interactions of MRSA and PAO1 Δ*pqsA* co-cultures via the GNPS platform (*18*). In the molecular network, the node representing *m/z* 339.0829

was within the molecular family of the *P. aeruginosa* produced siderophore pyochelin (*19*) (Pch, [M+H]+, calc 325.0681, *m/z* 325.0671, - 2.9525 ppm) and was annoted as pyochelin methylester (MetPch, [M+H]+, calc: 339.0837, m/z 339.0829, -2.4331 ppm). (**Fig. 1, B and C, and fig. S2**). This structural annotation of pyochelin and methyl ester pyochelin was confirmed by comparing the retention time, exact mass, and MS/MS fragmentation of the microbially produced metabolites to synthesized standards of both metabolites (**fig. S3, A and B**).

Co-cultures of MRSA with PAO1 Δ*pqsA* impaired in pyochelin biosynthesis (PAO1 Δ*pqsA* Δ*pch*) showed that loss of pyochelin production by PAO1 leads to loss of MetPch production (**Fig. 1D**). Although the spatial distribution of MetPch favored localization to the MRSA colony, several *P. aeruginosa* cystic fibrosis isolates have been shown to produce a methylated pyochelin (*20*). Therefore, to determine if MRSA methylates pyochelin, MRSA cultures were incubated with cell-free supernatant from PAO1 Δ*pqsA*, which includes Pch. Indeed, MRSA was responsible for methylation of pyochelin to MetPch (**fig. S4, A and B**).

To identify the gene encoding the enzyme responsible for conversion of Pch to MetPch in the *S. aureus* genome, we employed an LC-MS guided screen of the Nebraska Transposon Mutant Library (*21*) for loss of Pch methylation. After testing the first 700 clones of the transposon library, our analysis yielded a single transposon mutant, NE502 (transposon inserted in gene SAUSA300_1977), that was unable to produce MetPch. *In silico* analysis of the SAUSA300_1977 gene sequence identified it as encoding a putative methyltransferase (TcmP-like; IPR016874). Accordingly, from here, we will refer to SAUSA300_1977 as *spm* (staphylococcal pyochelin methyltransferase).

The gene encoding Spm is conserved across several *S. aureus* strains (**fig. S5, A and B**). MetPch production was observed exclusively from strains harboring the *spm* gene (strains

LAC, Newman, COL and MW2) while no MetPch production was detected by strains UAMS-1 and MN8, which do not encode the *spm* gene (**fig. S5C**). To further confirm that Spm is responsible for the methylation of Pch, a markerless in-frame deletion of *spm* (MRSA Δ*spm*) was incubated with cell free supernatant from PAO1 Δ*pqsA* and resulted in a significant decrease in detectable MetPch compared to MRSA wild-type (**Fig. 2A**). Genetic complementation of MRSA Δ*spm* with *spm* (MRSA Δ*spm*::*spm*) recovered production of MetPch to wild-type levels (**Fig. 2A**). This data confirms that Spm is necessary for the efficient generation of MetPch by *S. aureus*.

Spm is encoded in a putative operon downstream of the ferric uptake regulator (Fur) - regulated xenosiderophore receptor FhuD1 (*22, 23*). Closer examination of the *S. aureus* strains lacking the *spm* gene revealed the absence of the whole *fhuD1-spm* locus (**fig. S5B**). FhuD1 and FhuD2 are xenosiderophore receptors with a partially overlapping substrate range (*22*) and the xenosiderophores bound by these two receptors are transported into the *S. aureus* cells via the transporter machinery encoded by the *fhuGDE* operon (*24*). Based upon the proximity of *spm* to *fhuD1*, we tested whether the Fhu system was involved in MetPch production. Markerless in-frame deletions of *fhuD1* and *fhuD2* (MRSA Δ*fhuD1* Δ*fhuD2*) but not *fhuG* (MRSA Δ*fhuG*) showed increased MetPch generation (**Fig. 2B**). This data indicates that the Fhu system is most likely not involved in Pch or MetPch transportation, but FhuD1 and FhuD2 might bind Pch and exclude it from Spm-mediated methylation. In addition, the promoter driving the *fhuD1*/*spm* operon contains a predicted *fur* box (*22*) and its activity was significantly increased in a MRSA *fur* mutant (MRSA *fur::tet*) compared to wild-type (**fig. S6**), indicating MetPch production is dependent on Fur activity.

Pch exhibits antibacterial activity against *S. aureus*, a process that involves the production of intracellular reactive oxygen species (ROS) by *S. aureus* (*25*). MRSA treated with synthetic Pch, but not synthetic MetPch, had a concentration-dependent increase in ROS production

which was significantly higher than ROS produced by exposure to carrier control, for all tested concentrations (100, 200 and 400 µM) (**Fig. 2C**). High concentration of Pch inhibited *S. aureus* growth in an iron-limited environment, which was not observed with equimolar concentrations of MetPch (**fig. S7**).

The carboxylic acid moiety of pyochelin is required for iron binding as well as its interactions with its receptor (FptA) located on the outer membrane of *P. aeruginosa* (*26*). Therefore, methylation of the carboxylic acid of Pch could interfere with Pch-based iron acquisition by *P. aeruginosa*. Indeed, synthetic MetPch showed significantly lower iron binding than synthetic Pch measured via Chrom Azurol S (CAS) (**Fig. 2D**). To ascertain if reduced iron binding of MetPch leads to reduced growth support of *P. aeruginosa*, the siderophore activity of Pch and MetPch to support PAO1 growth under iron limited conditions was tested. Pyoverdine (Pvd) is a siderophore produced by *P. aeruginosa* with high affinity for iron (*27*). Only PAO1 deficient in the production of both siderophores (PAO1 Δ*pchF* Δ*pvdI*) is unable to grow under low iron conditions (M9 minimal medium supplementd with 500 µM 2,2′-Bipyridine), while production of either of the two PAO1 sideorphores is sufficient to support growth under the same conditions (**fig. S8**). While chemical complementation of PAO1 Δ*pchF* Δ*pvdI* with Pch was sufficient to recover *P. aeruginosa* growth to PAO1 Δ*pvdI* levels, MetPch was not (**Fig. 2E**). These results show that methylation of the carboxylic acid of Pch by *S. aureus* abrogates iron binding by Pch, which translates to decreases growth support of *P. aeruginosa.*

Taken together, our *in vitro* results show that *S. aureus* produces a methyltransferase that methylates the carboxylic acid moiety of Pch, which reduces *P. aeruginosa* Pch-mediated iron-acquisition and ROS production. This ability of *S. aureus* to diminish Pch bioactivity may represent a viable competition strategy for *S. aureus* to co-exist with *P. aeruginosa* during

co-infection *in vivo*. Therefore, microbial competition assays between PAO1 and MRSA, MRSA Δ*spm,* or MRSA Δ*spm*::*spm* were performed in a murine wound co-infection model.

As Spm is an uncharacterized enzyme, single infections with MRSA, MRSA Δ*spm,* or MRSA Δ*spm*::*spm* were performed and no significant changes in colony forming unit (CFU) recovery of the three MRSA strains were measured, demonstrating that Spm does not affect MRSA fitness in our *in vivo* model (**fig. S9**). However, in the co-infection model with PAO1, recovery of CFU of MRSA Δ*spm* was significantly reduced compared to MRSA and MRSA Δ*spm*::*spm*, indicating MRSA requires Spm for optimal fitness in a polymicrobial infection (**Fig. 3A**). Importantly, *P. aeruginosa* growth was similar for all co-infections (**Fig. 3B**). To determine if Spm is functionally active *in vivo*, the relative amount of Pch and MetPch was quantified from the skin wound tissue of the co-infection model. While Pch was measured from all co-infections in comparable amounts (**Fig. 3C**), MetPch levels were significantly lower in the co-infection of PAO1 with MRSA Δ*spm* (**Fig. 3D**). These results suggest that in the *in vivo* infection environment, *S. aureus* deactivates Pch through Spm-mediated methylation to enhance fitness in the presence of *P. aruginosa* and may contribute to co-existence in human infections.

The interaction of *S. aureus* and *P. aeruginosa* is multifaceted with contributions from temporal evolution of *P. aeruginosa* towards a less virulent phenotype during chronic infection and bioactivity of several metabolites, including HQNO, pyocyanin and rhamnolipids, contributing to the cooperation and antagonism between these two pathogens in the infection environment (*17*). Our investigation focused on the role of pyochelin, a metabolite that to date, has not been shown to have a direct impact on *S. aureus* and *P. aeruginosa* interaction during infection. We provide the first evidence that *S. aureus* harbors a system to deactivate the *P. aeruginosa* derived siderophore pyochelin by methylation via the enzyme Spm which translates to enhanced fitness of *S. aureus* in a wound co-infection model with *P. aeruginosa*.

Based upon the two-dimensional distribution of MetPch in the MALDI-MSI data and its lower abundance in tissue samples compared to Pch, we surmise that the deactivation of Pch is likely localized near *S. aureus* growth *in vivo*. Local methylation of Pch by *S. aureus* would result in two fitness benefits: increasing its own ability to acquire iron by impeding Pch iron binding and decreasing induction of its own ROS by detoxifying Pch. Interestingly, deactivation of Pch by esterification of the carboxylic acid moiety appears to be a conserved mechanism between a variety of microorganisms, including the fungus *Phellinus noxius* (*28*) and soil bacterium *Bacillus amyloliquefaciens* (*29*). However, the molecular and genetic mechanisms behind these biotransformation processes remain elusive. Pyochelin methylester has also been detected from CF sputum samples (*30*), indicating a possible role in bacterial competition in cystic fibrosis lungs. The apparent wide-spread mechanism by microbes from different kingdoms to deactivate Pch via chemical modification suggest that Pch may have a larger impact on microbial ecology than currently appreciated.

## References


1. C. F. F. P. Registry, 2019 Annual Data Report. *©2020 Cystic Fibrosis Foundation*, (2019).
2. K. Gjodsbol *et al.*, Multiple bacterial species reside in chronic wounds: a longitudinal study. *Int Wound J* **3**, 225-231 (2006).
3. C. B. Ibberson, M. Whiteley, The social life of microbes in chronic infection. *Curr Opin Microbiol* **53**, 44-50 (2020).
4. A. Korber *et al.*, Bacterial colonization of chronic leg ulcers: current results compared with data 5 years ago in a specialized dermatology department. *J Eur Acad Dermatol Venereol* **24**, 1017-1025 (2010).
5. L. J. Bessa, P. Fazii, M. Di Giulio, L. Cellini, Bacterial isolates from infected wounds and their antibiotic susceptibility pattern: some remarks about wound infection. *Int Wound J* **12**, 47-52 (2015).
6. D. H. Limoli, L. R. Hoffman, Help, hinder, hide and harm: what can we learn from the interactions between Pseudomonas aeruginosa and Staphylococcus aureus during respiratory infections? *Thorax* **74**, 684-692 (2019).
7. M. L. Maliniak, A. A. Stecenko, N. A. McCarty, A longitudinal analysis of chronic MRSA and Pseudomonas aeruginosa co-infection in cystic fibrosis: A single-center study. *J Cyst Fibros* **15**, 350-356 (2016).
8. J. W. Lightbown, F. L. Jackson, Inhibition of cytochrome systems of heart muscle and certain bacteria by the antagonists of dihydrostreptomycin: 2-alkyl-4-hydroxyquinoline N-oxides. *Biochem J* **63**, 130-137 (1956).
9. Z. A. Machan *et al.*, Interaction between Pseudomonas aeruginosa and Staphylococcus aureus: description of an anti-staphylococcal substance. *J Med Microbiol* **34**, 213-217 (1991).
10. L. Biswas, R. Biswas, M. Schlag, R. Bertram, F. Gotz, Small-colony variant selection as a survival strategy for Staphylococcus aureus in the presence of Pseudomonas aeruginosa. *Appl Environ Microbiol* **75**, 6910-6912 (2009).
11. R. Baldan *et al.*, Adaptation of Pseudomonas aeruginosa in Cystic Fibrosis airways influences virulence of Staphylococcus aureus in vitro and murine models of co-infection. *PLoS One* **9**, e89614 (2014).
12. S. DeLeon *et al.*, Synergistic interactions of Pseudomonas aeruginosa and Staphylococcus aureus in an in vitro wound model. *Infect Immun* **82**, 4718-4728 (2014).
13. Z. A. Machan, G. W. Taylor, T. L. Pitt, P. J. Cole, R. Wilson, 2-Heptyl-4-hydroxyquinoline N-oxide, an antistaphylococcal agent produced by Pseudomonas aeruginosa. *J Antimicrob Chemother* **30**, 615-623 (1992).
14. C. C. Caldwell *et al.*, Pseudomonas aeruginosa exotoxin pyocyanin causes cystic fibrosis airway pathogenesis. *Am J Pathol* **175**, 2473-2488 (2009).
15. A. V. Sotirova, D. I. Spasova, D. N. Galabova, E. Karpenko, A. Shulga, Rhamnolipid-biosurfactant permeabilizing effects on gram-positive and gram-negative bacterial strains. *Curr Microbiol* **56**, 639-644 (2008).
16. S. Heeb *et al.*, Quinolones: from antibiotics to autoinducers. *FEMS Microbiol Rev* **35**, 247-274 (2011).
17. L. Camus, P. Briaud, F. Vandenesch, K. Moreau, How Bacterial Adaptation to Cystic Fibrosis Environment Shapes Interactions Between Pseudomonas aeruginosa and Staphylococcus aureus. *Front Microbiol* **12**, 617784 (2021).
18. M. Wang *et al.*, Sharing and community curation of mass spectrometry data with Global Natural Products Social Molecular Networking. *Nat Biotechnol* **34**, 828-837 (2016).
19. Z. A. Youard, N. Wenner, C. Reimmann, Iron acquisition with the natural siderophore enantiomers pyochelin and enantio-pyochelin in Pseudomonas species. *Biometals* **24**, 513-522 (2011).
20. A. C. Lybbert, J. L. Williams, R. Raghuvanshi, A. D. Jones, R. A. Quinn, Mining Public Mass Spectrometry Data to Characterize the Diversity and Ubiquity of P. aeruginosa Specialized Metabolites. *Metabolites* **10**, (2020).

218 21. P. D. Fey *et al.*, A genetic resource for rapid and comprehensive phenotype screening of nonessential
219 Staphylococcus aureus genes. *mBio* **4**, e00537-00512 (2013).
220 22. M. T. Sebulsky, D. E. Heinrichs, Identification and characterization of fhuD1 and fhuD2, two genes
221 involved in iron-hydroxamate uptake in Staphylococcus aureus. *J Bacteriol* **183**, 4994-5000 (2001).
222 23. M. T. Sebulsky, C. D. Speziali, B. H. Shilton, D. R. Edgell, D. E. Heinrichs, FhuD1, a ferric hydroxamate-
223 binding lipoprotein in Staphylococcus aureus: a case of gene duplication and lateral transfer. *J Biol*
224 *Chem* **279**, 53152-53159 (2004).
225 24. M. T. Sebulsky, D. Hohnstein, M. D. Hunter, D. E. Heinrichs, Identification and characterization of a
226 membrane permease involved in iron-hydroxamate transport in Staphylococcus aureus. *J Bacteriol*
227 **182**, 4394-4400 (2000).
228 25. K. S. Ong, Y. L. Cheow, S. M. Lee, The role of reactive oxygen species in the antimicrobial activity of
229 pyochelin. *J Adv Res* **8**, 393-398 (2017).
230 26. D. Cobessi, H. Celia, F. Pattus, Crystal structure at high resolution of ferric-pyochelin and its
231 membrane receptor FptA from Pseudomonas aeruginosa. *J Mol Biol* **352**, 893-904 (2005).
232 27. I. J. Schalk, L. Guillon, Pyoverdine biosynthesis and secretion in Pseudomonas aeruginosa:
233 implications for metal homeostasis. *Environ Microbiol* **15**, 1661-1673 (2013).
234 28. Y. N. Ho *et al.*, Specific inactivation of an antifungal bacterial siderophore by a fungal plant pathogen.
235 *ISME J* **15**, 1858-1861 (2021).
236 29. C. Molina-Santiago *et al.*, Chemical interplay and complementary adaptative strategies toggle
237 bacterial antagonism and co-existence. *Cell Rep* **36**, 109449 (2021).
238 30. R. A. Quinn *et al.*, Neutrophilic proteolysis in the cystic fibrosis lung correlates with a pathogenic
239 microbiome. *Microbiome* **7**, 23 (2019).
240 31. H. J. Vogel, D. M. Bonner, Acetylornithinase of Escherichia coli: partial purification and some
241 properties. *J Biol Chem* **218**, 97-106 (1956).
242 32. Y. L. Yang, Y. Xu, P. Straight, P. C. Dorrestein, Translating metabolic exchange with imaging mass
243 spectrometry. *Nat Chem Biol* **5**, 885-887 (2009).
244 33. J. Y. Yang *et al.*, Primer on agar-based microbial imaging mass spectrometry. *J Bacteriol* **194**, 6023-
245 6028 (2012).
246 34. P. Shannon *et al.*, Cytoscape: a software environment for integrated models of biomolecular
247 interaction networks. *Genome Res* **13**, 2498-2504 (2003).
248 35. S. Noel, L. Guillon, I. J. Schalk, G. L. Mislin, Synthesis of fluorescent probes based on the pyochelin
249 siderophore scaffold. *Org Lett* **13**, 844-847 (2011).
250 36. J. D. Park, D. H. Kim, Cysteine derivatives as inhibitors for carboxypeptidase A: synthesis and
251 structure-activity relationships. *J Med Chem* **45**, 911-918 (2002).
252 37. K. L. Rinehart, A. L. Staley, S. R. Wilson, R. G. Ankenbauer, C. D. Cox, Stereochemical Assignment of
253 the Pyochelins. *The Journal of Organic Chemistry* **60**, 2786-2791 (1995).
254 38. B. R. Boles, M. Thoendel, A. J. Roth, A. R. Horswill, Identification of genes involved in polysaccharide-
255 independent Staphylococcus aureus biofilm formation. *PLoS One* **5**, e10146 (2010).
256 39. M. J. Horsburgh, E. Ingham, S. J. Foster, In Staphylococcus aureus, fur is an interactive regulator with
257 PerR, contributes to virulence, and Is necessary for oxidative stress resistance through positive
258 regulation of catalase and iron homeostasis. *J Bacteriol* **183**, 468-475 (2001).
259 40. B. W. Holloway, V. Krishnapillai, A. F. Morgan, Chromosomal genetics of Pseudomonas. *Microbiol*
260 *Rev* **43**, 73-102 (1979).
261 41. M. Toyofuku *et al.*, Influence of the Pseudomonas quinolone signal on denitrification in
262 Pseudomonas aeruginosa. *J Bacteriol* **190**, 7947-7956 (2008).
263 42. I. R. Monk, T. J. Foster, Genetic manipulation of Staphylococci-breaking through the barrier. *Front*
264 *Cell Infect Microbiol* **2**, 49 (2012).
265 43. J. L. Bose, P. D. Fey, K. W. Bayles, Genetic tools to enhance the study of gene function and regulation
266 in Staphylococcus aureus. *Appl Environ Microbiol* **79**, 2218-2224 (2013).
267 44. A. Rietsch, I. Vallet-Gely, S. L. Dove, J. J. Mekalanos, ExsE, a secreted regulator of type III secretion
268 genes in Pseudomonas aeruginosa. *Proc Natl Acad Sci U S A* **102**, 8006-8011 (2005).

## Acknowledgments

We thank Prof. Masanori Toyofuku, University of Tsukuba, for sharing *Pseudomonas aeruginosa* strains and Dr. Heidi Crosby for strain *S. aureus* LAC *fur*::tet.

**Funding:** Supported by Swiss National Science Foundation Early PostDoc mobility Fellowship P2ZHP3_168585 (CJ), NIH public health service grant AI083211 (ARH) and DE022350 (CM), and NIH NIGMS R35 GM128690 (VVP).

**Author Contributions:**

Conceptualization: CJ, VVP, ARH

Methodology: CJ, KK, JJ, MZ, KS, CM, VVP, ARH

Formal analysis: CJ, VVP

Investigation: CJ, KK, JJ, MZ, KS

Resources: CM, VVP, ARH

Data Curation: CJ, VVP

Writing Original Draft: CJ

Writing – Review & Editing: CJ, KK, JJ, MZ, KS, MS, CM, VVP, ARH

Visualization: CJ, KS, MZ

Supervision: CM, VVP, ARH

Funding Acquisition: CJ, CM, VVP, ARH

**Competing interests:** Authors declare that they have no competing interests

**Data and Matrials Availability:** All mass spectrometry data, including the raw files, mzXML files, metadata tables and MZmine settings are available via MassIVE (MSV000089230; *P. aeruginosa*/*S. aureus* wt, *spm* mutant, *spm* complementation interaction, MSV000089231; *P. aeruginosa*/*S. aureus* wt, *fhuG* mutant, *fhuD*1/*D*2 double mutant interaction, MSV000089233, Pyochelin methylation by *S. aureus* transposon library mutants, MSV000089234; Pyochelin methylester quantification murine skin wound model *S. aureus*/*P. aeruginosa* co-infection).

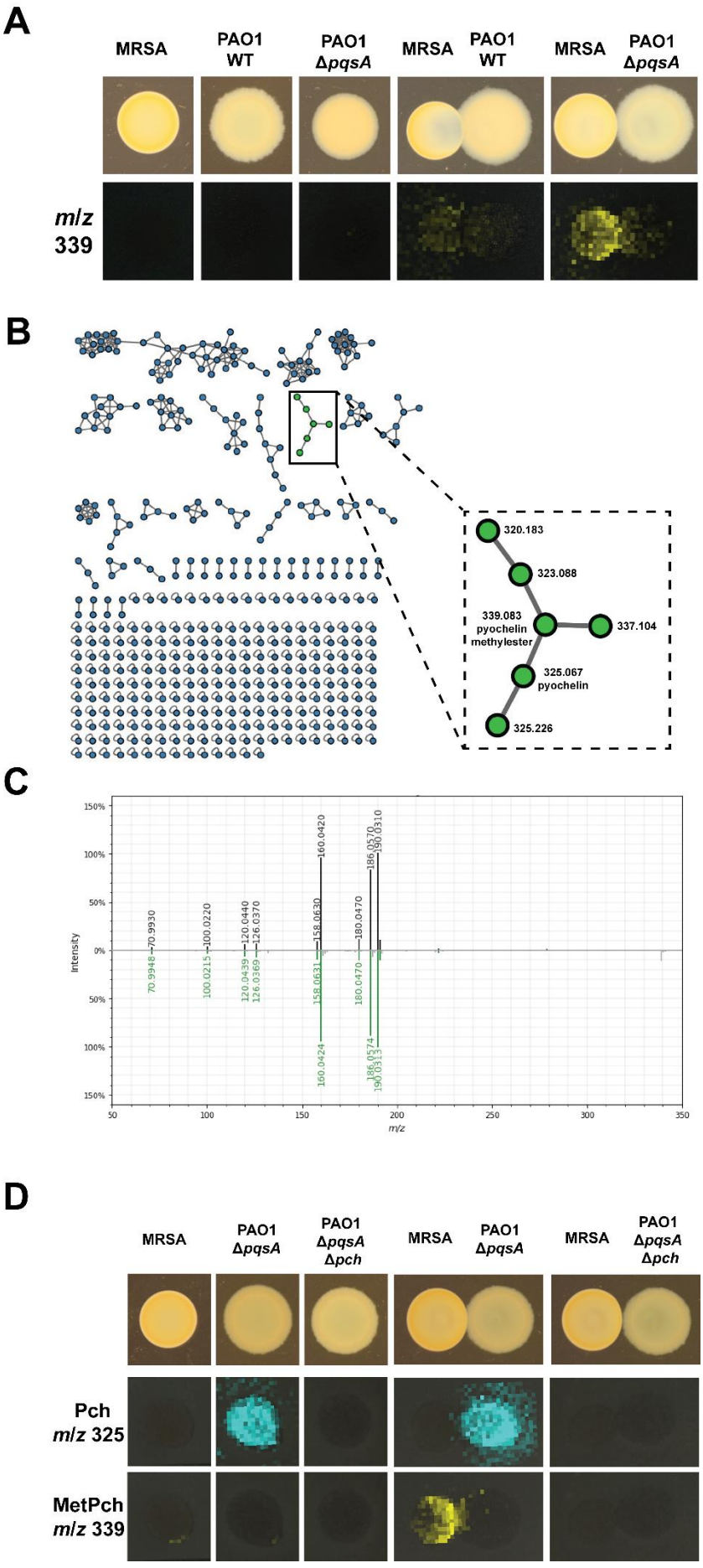
A
MRSA
PAO1 WT
PAO1 ΔpqsA
MRSA
PAO1 WT
MRSA
PAO1 ΔpqsA
m/z 339
B
320.183
323.088
339.083 pyochelin methylester
337.104
325.067 pyochelin
325.226
C
Intensity
m/z
D
MRSA
PAO1 ΔpqsA
PAO1 ΔpqsA Δpch
MRSA
PAO1 ΔpqsA
MRSA
PAO1 ΔpqsA Δpch
Pch m/z 325
MetPch m/z 339

296

**Figure 1:** Pyochelin methylester (MetPch) is produced during interaction of *S. aureus* and *P. aeruginosa* **A)** MALDI-MSI of *S. aureus* and *P. aeruginosa* grown as mono cultures or interactions. Photographs of the cultures before matrix application are shown on top. *P. aeruginosa* wildtype (PAO1 WT) but not a *P. aeruginosa* quinolone mutant (PAO1 Δ*pqsA*) inhibits *S. aureus* wildtype (MRSA) when grown in co-cultures. The bottom row shows the false colored *m/z* distribution of an unknown compound with *m/z* 339 that was exclusively observed during interaction of *P. aeruginosa* and *S. aureus*. **B**) The interaction specific compound (*m/z* 339) is annotated as pyochelin methylester (MetPch), a member of the pyochelin (Pch) molecular family, by molecular networking. **C)** Mirror plot comparing the $MS^2$ spectrum of isolated MetPch (top; black trace) with its GNPS library match (bottom; green trace). **D)** MALDI-MSI of *S. aureus* and *P. aeruginosa* producing (Δ*pqsA*) or not producing pyochelin (Δ*pqsA* Δ*pch*). Photographs of the cultures before matrix application are shown on top. The middle row shows the false colored m/z distribution for Pch (*m/z* 325) and the bottom row for MetPch (*m/z* 339). Pch production can be observed by PAO1 Δ*pqsA*, but not PAO1 Δ*pqsA* Δ*pch*.

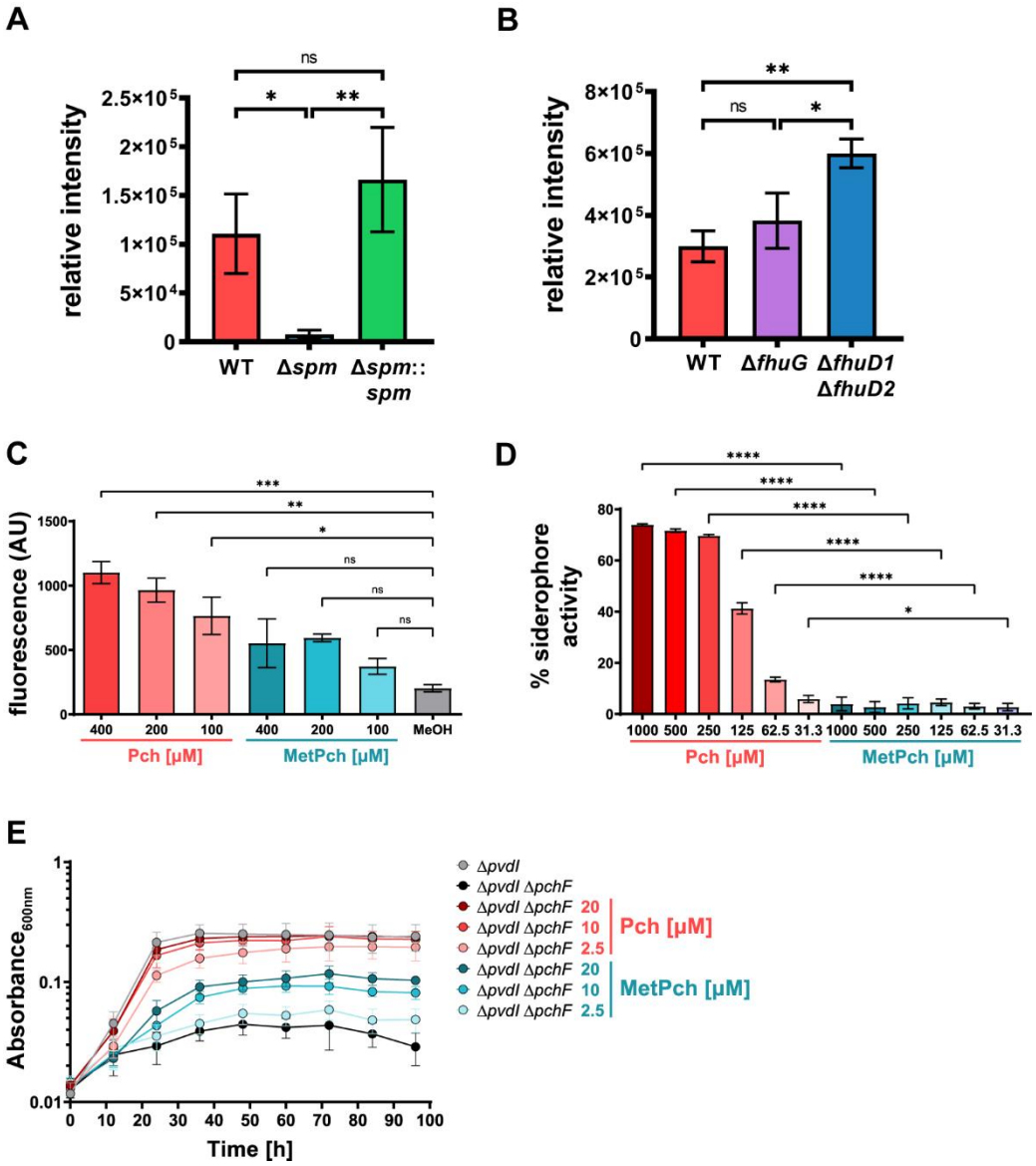


**Figure 2:** Spm mediated methylation leads to Pch inactivation. **A)** Incubation of PAO1 Δ*pqsA* cell-free supernatant with overnight cultures of MRSA wildtype (WT), an *spm* mutant strain (Δ*spm*) and its corresponding complementation strain (Δ*spm*::*spm*) results in high amounts of MetPch production by MRSA WT and MRSA Δ*spm*::*spm* but not by MRSA Δ*spm*. n = 3 biological replicates. [one-way ANOVA with Tukey's multiple comparison] **B)** The Fhu xenosiderophore uptake machinery does not promote MetPch production. Mutation of the two xenosiderophore receptors *fhuD1* and *fhuD2 (ΔfhuD1 ΔfhuD2)* but not *fhuG* (Δ*fhuG*), which is essential for the uptake of several hydroxamate xenosiderophores, does result in significantly lowered MetPch production. n = 3 biological replicates. [one-way ANOVA with

Tukey's multiple comparison] **C)** Exposure to Pch but not MetPch results in significantly elevated ROS production of MRSA WT compared to the carrier control (MeOH). Numbers indicated the µM concentration of Pch and MetPch used in the experiment. n = 3 biological replicates. [Kruskal-Wallis with Dunn's multiple comparison] **D)** Siderophore activity of Pch and MetPch were evaluated by liquid Chrome Azural S assay for concentrations ranging from 31.25 to 1000 µm. Siderophore activity of MetPch is significantly reduced compared to Pch across all tested concentrations. n = 5 biological replicates. [one-way ANOVA and Šidák's multiple comparison] **E)** Pch but not MetPch supports *P. aeruginosa* growth under low iron conditions. 96-hour growth curves of a *P. aeruginosa* PAO1 pyoverdine mutant (Δ*pvdI*) and a pyoverdine/pyochelin double mutant (Δ*pvdI* Δ*pchF*) supplemented with different concentrations of synthetic Pch or MetPch. Cultures were grown in M9 minimal medium with glycerol as carbon source. To create a low iron environment, 500 µM 2,2'-Bipyridine was added to the growth medium. n = 5 biological replicates from 4 independent experiments **A – D)** Values are mean ± SDs. *$P \leq 0.05$, **$P \leq 0.01$, ***$P \leq 0.001$, ****$P \leq 0.0001$, ns = not significant.

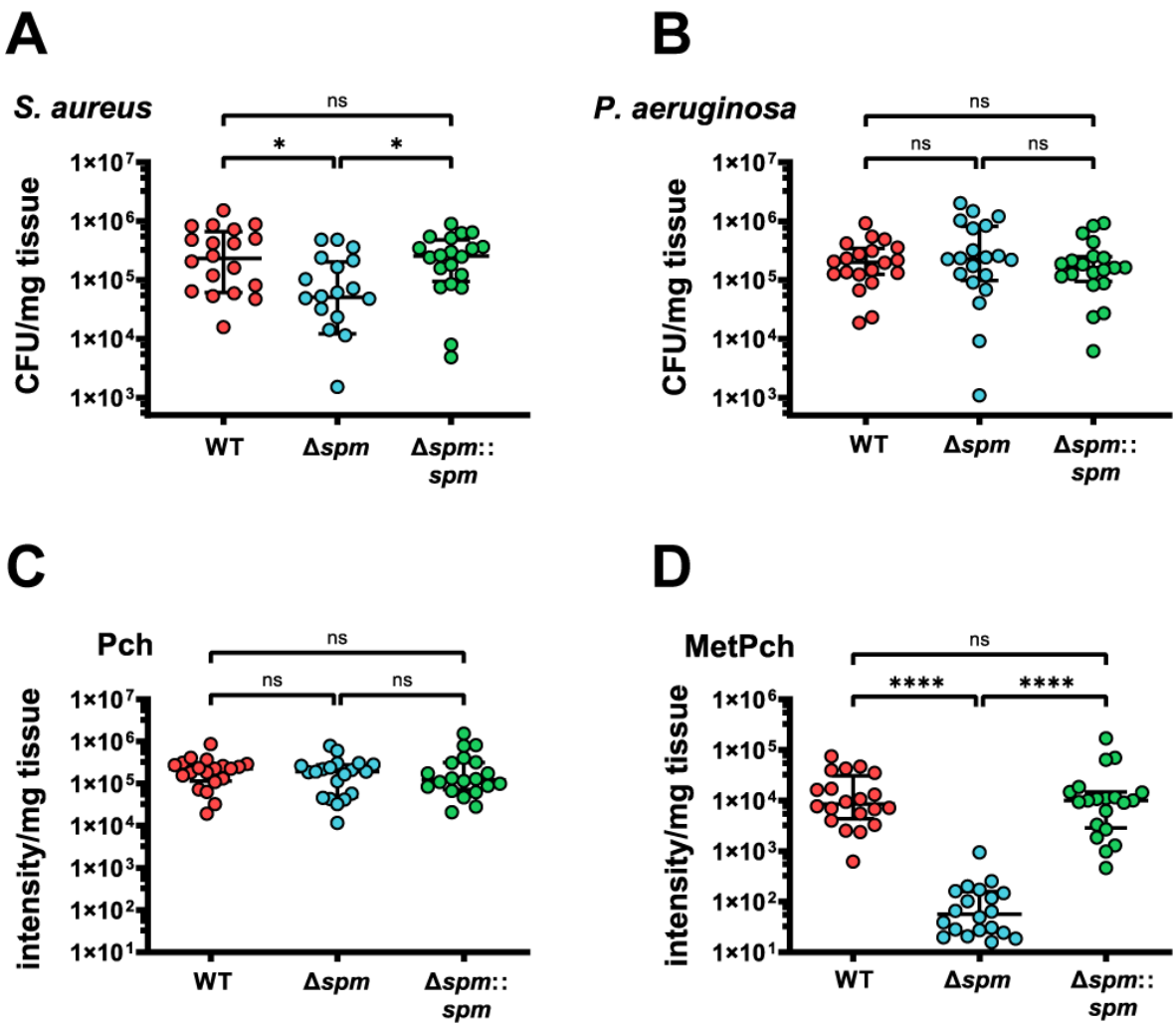


**Figure 3:** Mutation of *spm* impairs the fitness of MRSA during co-infection with PAO1. **A**) MRSA CFUs recovered from mouse tissues. **B**) *P. aeruginosa* CFUs recovered from mouse tissues. **C)** quantification of Pch and **D)** MetPch recovered from mouse tissue co-infected with PAO1 (WT) and MRSA. All co-infections were performed with *P. aeruginosa* PAO1 wildtype and either MRSA wildtype (WT), the Spm mutant strain (Δ*spm*) or the Spm complemented strain (Δ*spm*::*spm*). The co-infecting MRSA strain is indicated below the X-axis. n = 20 biological replicates from 4 independent experiments. [Kruskal-Wallis with Dunn's multiple comparison] **A – D**) Values are median ± interquartile range. Each dot represents values from a single mouse. **P* ≤ 0.05, ***P* ≤ 0.01, ****P* ≤ 0.001, *****P* ≤ 0.0001, ns = not significant.

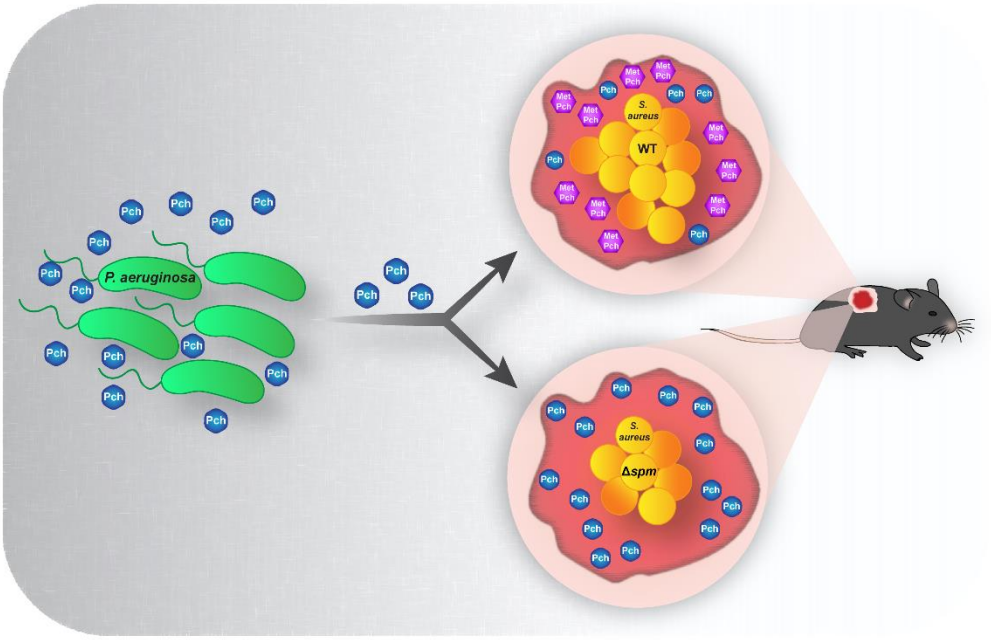


**Figure 4:** Model of *S. aureus*/*P. aeruginosa* chemical interaction. *P. aeruginosa* produces and secretes pyochelin during infection. *S. aureus* wild type cells inactivate pyochelin through enzymatic methylation. *S. aureus* mutant cells lacking the Spm methyltransferase are unable to methylate pyochelin. Pyochelin methylation leads the loss of siderophore activity and reduced intracellular ROS production in *S. aureus* cells, resulting in a higher fitness of *S. aureus* during competition with *P. aeruginosa in vivo*.